

# Cross-Antenna Polyphase Interleaving and Inversion scheme to reduce the PAPR of MIMO-FBMC/OQAM system

Mounira Laabidi, and Ridha Boualleguee

**Abstract**—Filter Bank Multi-Carrier with Offset Quadrature Amplitude symbol mapping called as FBMC/OQAM is presented as a potential successor of Orthogonal Frequency Division Multiplexing OFDM. Combined with Multiple-Input Multiple-Output (MIMO), MIMO-FBMC/OQAM is a promising modulation scheme for high performance broadband wireless communications. However, one major drawback of MIMO-FBMC/OQAM is the high peak-to-average power ratio (PAPR) of the output signals. Latinovic et al. Proposed a PAPR reduction method called Polyphase Interleaving and Inversion (PII) for MIMO-OFDM systems under the use of the space-frequency block coding (SFBC) [1]. In this investigation, we suggest two schemes called Cross Antenna Polyphase Interleaving and Inversion 1 and 2 (CAPII1/CAPII2) PAPR reduction schemes for Space Frequency Block Coding MIMO-FBMC systems which consequently utilizes additional degrees of freedom by employing multiple antennas and generating more patterns leading to more signal candidates to transmit, while requiring a limited amount of side information. The simulation results show that both the proposed CAPII schemes experience remarkable gain in PAPR.

**Keywords**—Multiple-Input Multiple-Output (MIMO); FBMC/OQAM; Peak-to-Average Power Ratio (PAPR); Space-Frequency Block Coding (SFBC); CAPII

## I. INTRODUCTION

IN the last decade, Orthogonal frequency division multiplexing (OFDM) has been widely used in 4G communication systems [2], [3], [4], [5]. This is because of its important features such as (i) immunity to multipath fading, (ii) ease of channel estimation also data recovery with a low complexity single tap equalization, and (iii) appropriateness for multiple-input multiple-output (MIMO) systems. Nevertheless, it reveals many drawbacks such as cyclic prefix over-head, considerable out-of-band (OOB) radiation, and sensitivity to carrier frequency offset (CFO) leading to inter carriers interference (ICI). Because of the OFDM shortcomings [6], Filter Bank Multicarrier with Offset Quadrature Amplitude Modulation System (FBMC/OQAM) is one of many new waveforms that are proposed for the next 5G wireless communication applications due to its attractive properties and features related to spectral confinement [7], [8]. With a well localized prototype filters in time and frequency domain for pulse

This work was supported by the Innov'COM Laboratory of Higher School of Telecommunication (Sup'Com), University of Carthage Tunisia. Authors are with Sup'Com, University of Carthage, Tunisia (e-mail: mounira.laabidi@supcom.tn, ridha.boualleguee@supcom.tn).

shaping, FBMC/OQAM not only provides notably reduced Out Of Band (OOB) emissions and robustness against Carrier Frequency Offset (CFO), but also, better spectral efficiency since there is no need to use the over-head of cyclic prefix. To improve the performance of wireless communication systems and increase its capacity, multiple antennas at both the transmitter and receiver can be used (MIMO) [9]. MIMO technology is used for wifi networks, forth generation (4G) applications and (5G) technology in a wide range of markets.

When combined with FBMC/OQAM, this MIMO system leads to robustness to multipath fading [10], [11], high capacity, and upgraded spectral efficiency making from FBMC/OQAM a high-data speed multicarrier transmission in forthcoming wireless communication network systems [12], [13], [14], [15].

However, a major drawback of MIMO technology combined with the FBMC/OQAM system is that the transmitted signals on different antennas might exhibit a prohibitively large peak-to-average power ratio (PAPR) [16] due to the summation of independent information carried on different subcarriers.

In the existing literature, various methods have been introduced to address the high Peak-to-Average Power Ratio (PAPR) associated with Single-Input Single-Output (SISO) FBMC/OQAM signals. These methods include clipping [17], Partial Transmit Sequence (PTS) [18], Selective Mapping (SLM) [19], Interleaving, Active Constellation Extension (ACE) [20], Tone Reservation (TR) [21], Tone Injection (TI) [22], companding techniques [23], and precoding techniques [24]. However, when it comes to mitigating the high PAPR specifically in Multiple-Input Multiple-Output (MIMO) Space-Frequency Block Code (SFBC) FBMC/OQAM signals, there is a notable scarcity of works addressing this particular issue. In [25], authors proposed new schemes to reduce PAPR for MIMO STBC FBMC system. The scheme is a combination of Walsh-Hadamard Transform (WHT) precoding with the companding technique based on the A-law and Mu-law technique. the proposed technique achieves PAPR reduction at the expense of degrading BER performance

In [26] a scheme named Attenuating Quadrature Amplitude Modulation Symbols (AQAMS) with MIMO system is proposed to reduce the PAPR of the FBMC-OQAM signal. Simulation findings following the AQAMS technique illustrate concrete progress regarding PAPR reduction. However, as a



limitation of this scheme the amount of side information that need to be transmitted to the receiver in order to recover data.

In [27], authors advanced a new PAPR reduction method for MIMO FBMC/OQAM system based on the iterative addition and subtraction of FBMC/OQAM symbols which is known as Successive Addition Subtraction (SAS) followed by the WHT precoding. Simulation results show that the proposed schemes can improve the performance of the transceiver.

In [28] authors suggested a Repeated Clipping Filtering combined with several Nonlinear Companding techniques including A-Law, Mu-Law, tangente rooting (tanhR), logarithmic rooting (logR), cos and rooting companding (RTC) for PAPR Reduction in MIMO FBMC/OQAM System). Yet, these methods may increase the Bit Error Rate (BER) of the system given that clipping is a nonlinear process.

In [1] S. Latinović et al. proposed a PAPR reduction method termed polyphase interleaving and inversion (PII) for MIMO-OFDM systems under the use of SFBC. The suggested scheme uses four patterns to present data over the two antenna. In this investigation, we find more degrees of freedom can be utilized among the multiple antennas for the SFBC MIMO FBMC/OQAM systems. Hence, we suggest four additional SFBC patterns, and based on these patterns, we propose two new efficient PAPR reduction schemes for SFBC MIMO-FBMC/OQAM systems. The Cross Antenna Polyphase Interleaving and Inversion (CAPII) method operates by adjusting the phase of the data symbols and swaps data symbols between two antennas to reduce the PAPR.

The organization of this paper is as follows: In section 2, we survey the implementation structures of the FBMC/OQAM and the MIMO SFBC Alamouti scheme. In section 3, at first a brief reminder of the PII PAPR reduction scheme being suggested for MIMO OFDM is done. Then, the proposed two CAPII reduction schemes, to improve the PAPR of the MIMO SFBC FBMC/OQAM is introduced. Section 4, reports the simulation results with regard to the performances of the proposed schemes. This section includes the discussion of the obtained results. Finally, conclusions and perspectives are stated in section 5.

## II. THEORY

In this section, we survey the implementation structures of the FBMC/OQAM and the MIMO SFBC Alamouti scheme.

### A. FBMC/OQAM signal model

FBMC/OQAM is an alternative modulation scheme to replace the traditional OFDM (Orthogonal Frequency Division Multiplexing). It uses a bank of filter to divide the available frequency band into multiple subbands, each with its own subcarrier. Symbols are OQAM modulated, and the offset between the real and imaginary parts of the signal allows for a more flexible and efficient use of the frequency spectrum compared to traditional QAM.

FBMC/OQAM highlights the merits of the promising modulation scheme for 5th generation (5G) communication system. The basic idea of FBMC/OQAM system is to transmit real symbols (Offset QAM) instead of conventional

complex (QAM) symbols like in OFDM system. Thus, on each sub-channel the sequence of QAM symbols is divided into real and imaginary parts, and upsampled by a factor of two to obtain the real sequences. That is, the in-phase and quadrature components of QAM symbols are times staggered by half a symbol period  $T/2$ . We can refer to this operation as OQAM pre-processing. Another specificity of the FBMC/OQAM scheme is that when we consider two consecutive sub-carriers, the time delay  $T/2$  is introduced into the imaginary part of the QAM symbols on the even subcarrier, whereas it is introduced into the real part of the symbols on the odd one as shown in Figure 1.

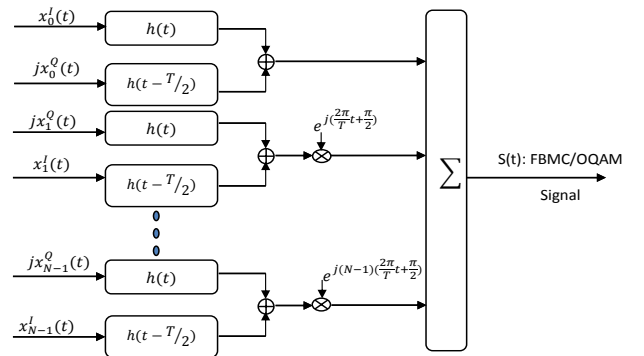


Fig. 1. FBMC/OQAM Transmitter.

The integral components of the FBMC/OQAM Transmultiplexer (TMUX) include the Synthesis filter bank (SFB) on the transmitter side and the Analysis filter bank (AFB) on the receiver side. The SFB plays a crucial role in ensuring that OQAM sequences undergo both spreading and filtering processes.

Pulse shaping in FBMC/OQAM is accomplished by the prototype filter, which comes in two main types: the Isotropic Orthogonal Transform Algorithm-based pulse (IOTA) [29] and the pulse utilized in the PHYDYAS project [30]. This study focuses specifically on the PHYDYAS prototype filter.

The SFB is constructed by combining the PHYDYAS prototype filter with an extended Inverse Fast Fourier Transform (IFFT). This configuration not only achieves orthogonality without relying on Cyclic Prefixes (CPs) but also demonstrates enhanced spectral efficiency, high bandwidth efficiency, and increased channel capacity [31].

Consequently, the following equation defines the baseband continuous-time model of the FBMC/OQAM transmitted signal:

$$s(t) = \sum_{m=0}^{N-1} \sum_{n=-\infty}^{\infty} a_{m,n} h\left(t - n\frac{T}{2}\right) e^{j\frac{2\pi}{T}mt} e^{j\varphi_{m,n}} \quad (1)$$

where:

- $a_{m,n}$  is a real symbol transmitted on the  $m$ th sub-carrier and at the instant  $nT$ ,
- $h(t)$  is the prototype filter impulse response, and

- $\varphi_{m,n}$  is the phase term which is given by the following equation:

$$\varphi_{m,n} = \frac{\pi}{2}(m+n) - \pi(mn) \quad (2)$$

If we denote  $\Upsilon_{m,n}(t)$  as the prototype's filter  $h(t)$  shifted version in time and frequency, therefore the baseband continuous-time model of the FBMC/OQAM transmitted signal can be rewritten as follows:

$$s(t) = \sum_{m=0}^{N-1} \sum_{n=-\infty}^{\infty} a_{m,n} \Upsilon_{m,n}(t) \quad (3)$$

where

$$\Upsilon_{m,n}(t) = h\left(t - n\frac{T}{2}\right) e^{j\frac{2\pi}{T}mt} e^{j\varphi_{m,n}} \quad (4)$$

In this investigation, we have opted for the PHYsical layer for DYnamic AccesS and cognitive radio prototype Filter (PHYDYAS), an advanced filter proposed by Bellanger in [32]. This selection is motivated by several factors. Primarily, the outstanding frequency localization characteristic of FBMC/OQAM systems is effectively addressed by the PHYDYAS prototype filter, aligning well with the system's requirements. Additionally, in comparison to the Isotropic Orthogonal Transform Algorithm (IOTA) filter, the PHYDYAS prototype filter exhibits superior spectral efficiency, attributed to its design grounded in the frequency sampling technique, as highlighted in [30]. The PHYDYAS European project has designated the PHYDYAS prototype filter as the benchmark prototype filter. Key parameters governing the design of the filter bank include the number of sub-channels denoted as  $N$  and the prototype filter length, designated as  $L$ . The prototype filter length is consistently determined through a multiplication operation involving both  $N$  and the overlapping factor  $K$ . Specifically, for the PHYDYAS filter, the relationship is expressed as  $L = K * N$ .

Despite the big number of benefits that it offers being an MCM scheme, FBMC/OQAM signal suffers from the high PAPR which is noticeable when there is a non-linear HPA. In the following part, the PAPR definition for the FBMC/OQAM signal is advanced.

### B. PAPR definition for FBMC/OQAM signal

The Peak-to-Average Power Ratio (PAPR) serves as a crucial metric for assessing the susceptibility of the transmitted signal, particularly in the presence of a fluctuating envelope due to High Power Amplifier (HPA) non-linearity. In the realm of Multi-Carrier Modulation (MCM) systems, the inherent high PAPR poses a significant challenge in designing HPAs that need to operate within their linear regions. Additionally, the PAPR acts as a pivotal parameter when comparing the effectiveness of various PAPR reduction schemes, playing a key role in evaluating their capability to reduce signal peaks. Small PAPR values signify that the transmitted signal consistently hovers around its mean power, whereas large PAPR values indicate that the instantaneous power can markedly surpass the average power. The PAPR of the continuous-time baseband

signal  $s(t)$  transmitted within a symbol period  $T$  is formally defined as equation(5):

$$PAPR_{[s]} = \frac{\max_{n \in [0, N-1]} |s(n)|^2}{E[|s(n)|^2]} \quad (5)$$

Where  $E[\cdot]$  is the expectation operator and  $s(n)$  is the MCM symbol. In OFDM, symbols are isolated in the time domain, i.e., they do not overlap. Subsequently the PAPR calculation is achieved for every symbol exactly in its symbol period. Whereas, due to its overlapping signal structure, the PAPR calculation of an FBMC/OQAM signal should be calculated on a period rather than in its own designated interval. As concluded in [33] the illustration reveals that, for a given FBMC/OQAM symbol, a significant portion of its energy is concentrated in the  $2^{nd}$  and  $3^{rd}$  time intervals, rather than in its own designated interval

### C. Alamouti SFBC principle

To achieve diversity and upgrade the reliability of the communication link in wireless communications, Alamouti Space-Time Block Coding (STBC) transmission technique is used. STBC is specifically convenient in Multiple Input Multiple Output (MIMO) systems. Alamouti STBC was advanced by Professor Siavash Alamouti in 1998 [34] and is definitely designed for two transmit antennas. MIMO systems use multiple antennas at both the transmitter and receiver to improve the data throughput and reliability of wireless communication. The central idea behind Alamouti STBC is to transmit two symbols over two consecutive time intervals using two antennas, and then apply a simple coding scheme to these symbols before transmission. The encoding is done in such a way that the information from both symbols is spread through both antennas. The encoded symbols are then transmitted from the two antennas. At the receiver side, the combination of the received signals from the two antennas is accomplished to take advantage of the diversity provided by the two spatially separated antennas. The Alamouti code matrix for the two symbols  $X_1$  and  $X_2$  is as follows:

At the first time slot, the symbols  $X_1$  and  $X_2$  are transmitted respectively on the antennas 1 and 2 then at the second time slot, the symbols  $-X_2^*$   $X_1^*$  are transmitted on the antennas 1 and 2 and so on...

Where  $X_1^*$  is the complex conjugate of  $X_1$  and  $X_2^*$  is the complex conjugate of  $X_2$ .

Applied to the frequency domain instead of the time domain, the resulting Alamouti block coding is called Space-Frequency Block Code (SFBC) where two consecutive and neighboring subcarriers within the same symbol are considered instead of two consecutive time slots. In this investigation, we are interested in SFBC Alamouti scheme since the STBC Alamouti requires complex orthogonality and the FBMC/OQAM signal is only real-orthogonal.

## III. CAPII METHOD TO REDUCE THE PAPR OF THE MIMO FBMC/OQAM

### A. Conventional PII scheme

Polyphase Interleaving and Inversion (PII) scheme [1] is an efficient PAPR reduction approach being suggested for

TABLE I  
SPACE FREQUENCY BLOCK ENCODING

	Antenna 1	Antenna 2
f1	$X_1$	$X_2$
f2	$-X_2^*$	$X_1^*$

SFBC MIMO-OFDM systems. This method reduces PAPR of the transmit signal while keeping the space-frequency coded structure. Polyphase interleaving involves distributing symbols intended for transmission across various subcarriers in a specific interleaved pattern. This process serves to disperse the energy of the transmitted signal across the entire bandwidth, thereby diminishing the probability of simultaneous high peaks occurring across all subcarriers. The application of polyphase interleaving contributes to the even distribution of energy among subcarriers, and inversion is selectively employed to mitigate peaks in specific regions.

The principle of PII is as follows: the OFDM data block is firstly partitioned into  $M$  disjoint subblocks  $X(m), m = 1, 2, \dots, M$ . In each subblock, the data are interleaved and inverted across the antennas to produce four different SFBC signal models to transmit across antenna 1 and 2. Where  $b_m X_1^{(r_m)}$  and  $b_m X_2^{(r_m)}$  respectively represent the  $m^{th}$  subblocks of the candidate transmit signals for antenna 1 and antenna 2. The values of  $b_m$  and  $r_m$  specify one SFBC pattern from four possible patterns ( $b_m = [+1, -1], r_m = [0, 1]$ ).

The conventional space-frequency Alamouti scheme is described when the values of ( $b_m = 1$ ) and ( $r_m = 0$ ). Table II shows an example of these models.

TABLE II  
THE FOUR TYPES OF SFBC PATTERNS USED IN PII METHOD

Pattern 1	Pattern 2
$X_1^0(m) = [X_0 - X_1^*]$	$-X_1^0(m) = [-X_0 X_1^*]$
$X_2^0(m) = [X_1 X_0^*]$	$-X_2^0(m) = [-X_1 - X_0^*]$
Pattern 3	Pattern 4
$X_1^1(m) = [X_1 - X_0^*]$	$-X_1^1(m) = [-X_1 X_0^*]$
$X_2^1(m) = [X_0 X_1^*]$	$-X_2^1(m) = [-X_0 - X_1^*]$

### B. Proposed CAPII schemes for SFBC MIMO-FBMC/OQAM

Examining the PII PAPR reduction scheme and reviewing the four SFBC patterns outlined in Table 1, it becomes apparent that these patterns result from interleaving across antennas and the inversion of element signs. Notably, these patterns maintain the space-frequency coded structure characteristic of Alamouti, ensuring the preservation of diversity gains from multiple antennas.

The fundamental concept behind the CAPII scheme lies in generating additional sets of candidate patterns for selection. This approach aims to enhance PAPR reduction performance by providing a broader range of choices for pattern selection. Table III describes the additional four models.

Concerning the CAPII1 PAPR reduction scheme, We select patterns 1,6, 7 and 8. We can recognize that for each antenna

TABLE III  
THE FOUR ADDITIONAL TYPES OF SFBC PATTERNS

Pattern 5	Pattern 6
$[-X_1^* X_0]$	$[-X_1^* - X_0]$
$[X_0^* X_1]$	$[X_0^* - X_1]$
Pattern 7	Pattern 8
$[-X_0 - X_1^*]$	$[X_0 X_1^*]$
$[X_1 - X_0^*]$	$[-X_1 X_0^*]$

and based on the PII principle, a symbol is partitioned into two subblocks, and each subblock has four space-frequency (SF) coding patterns. Hence, the CAPII1 method in this case generates 16 sets of candidate signals for antenna 1 and 2, and it selects the best set (the best PAPR reduction performance) for transmission.

Based on the same principle, CAPII2 PAPR reduction scheme reduces the high PAPR of the SFBC MIMO FBMC/OQAM signal by generating more and more signal candidate for transmission since it utilises all the 8 patterns. Thereby, it can produce sixty four signal candidates and ensure remarkable gain of PAPR when compared to the PII scheme or even to the CAPII1 technique. Fig.??illustrates the position and principle of the CAPII2 scheme on the MIMO FBMC/OQAM transmission chain.

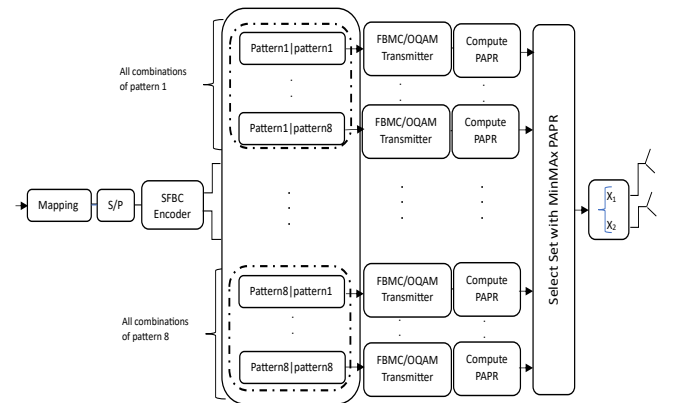


Fig. 2. The graphical illustration of the CAPII2 PAPR reduction scheme for SFBC MIMO FBMC/OQAM system

## IV. EXPERIMENT

In this section we examine the performance of both MIMO FBMC/OQAM and MIMO OFDM systems. To do so, we developed a simulation model using MATAB. Simulation parameters are shown in Table IV.

The PAPR reduction capabilities of the above-mentioned two CAPII method (i.e. CAPII1 and CAPII2) being suggested for MIMO FBMC/OQAM are verified through simulations. To understand the effectiveness of the scheme under various conditions, the complementary cumulative distribution function (CCDF) diagrams of the CAPII techniques, and the complexity all being used to compare both MIMO FBMC/OQAM and MIMO OFDM systems..



TABLE IV  
SIMULATION PARAMETERS

Parameter	Value
FFT size, N	64
Modulation order, M	2
Cyclic Prefix, Cp	N/8
Number of PII patterns	4
Number of CAPII1 patterns	4
Number of CAPII2 patterns	8
Modulation scheme	QAM
Filter	PHYDYAS
Overlapping factor $K$	4
Filter Length, L	43

A. CCDFs comparisons

In this sub-section we evaluate the performance of both CAPII PAPR reduction schemes being suggested for SFBC MIMO FBMC/OQAM in terms of CCDFs. We also, compare their PAPR reduction gain with the advanced PII scheme.

The CCDFs plot of both SISO and MIMO FBMC/OQAM systems without PAPR reduction are illustrated in Fig.3. We can recognize that the MIMO FBMC/OQAM CCDF curve ensures a reduction of approximately 1.1 [dB] at a probability level of  $10^{-3}$  with respect to SISO FBMC/OQAM. This result can be explained as the diversity gain.

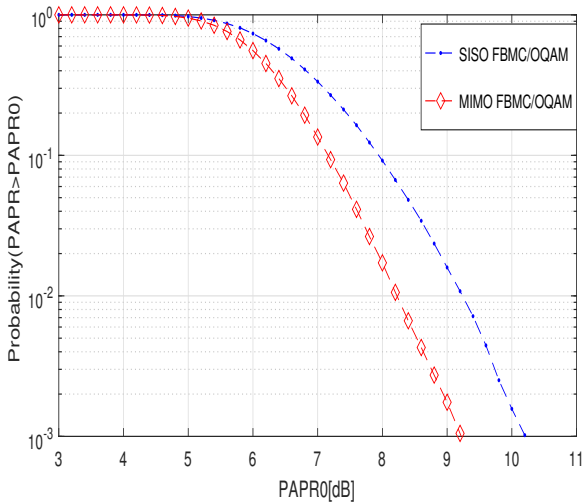


Fig. 3. CCDF comparison between SISO FBMC/OQAM and MIMO FBMC/OQAM

To demonstrate the effectiveness of the being suggested CAPII PAPR reduction schemes (CAPII1 and CAPII2), a simulation based on the PII scheme is useful. Hence, Fig.4 illustrates the CCDFs of MIMO FBMC/OQAM signal with and without applying the PII PAPR reduction method. As it is clear from the figure below, at a probability level of  $10^{-3}$  the PII PAPR reduction gain is approximately 2.6 [dB] with respect to the MIMO FBMC/OQAM signal without PAPR reduction.

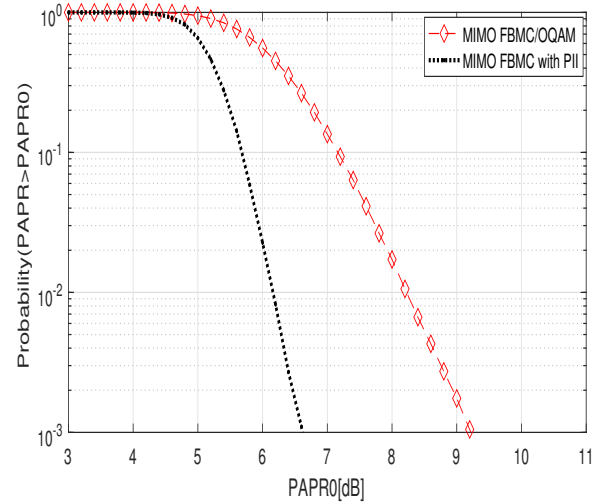


Fig. 4. PAPR performance of the PII scheme when applied to SFBC MIMO-FBMC/OQAM

Fig.5 illustrates the CCDFs of MIMO FBMC/OQAM signal when applying the CAPII PAPR reduction methods. It also, provides a comparison with the PII scheme.

At a CCDF level of  $10^{-3}$  [dB], the PAPR reduction gain is detailed in Table V. Examination of the table reveals that the PAPR reduction performance of both PII and CAPII1 is very similar, attributable to their utilization of four SFBC patterns. Looking at the CAPII2 PAPR reduction scheme, it outperforms both CAPII1 and PII schemes. In comparison to the original MIMO FBMC/OQAM signal without a PAPR reduction scheme, the CAPII2 method achieves a PAPR gain of approximately 4 dB. This outcome can be attributed to the substantial number of SFBC MIMO FBMC/OQAM signal candidates, as the scheme incorporates all eight SFBC patterns.

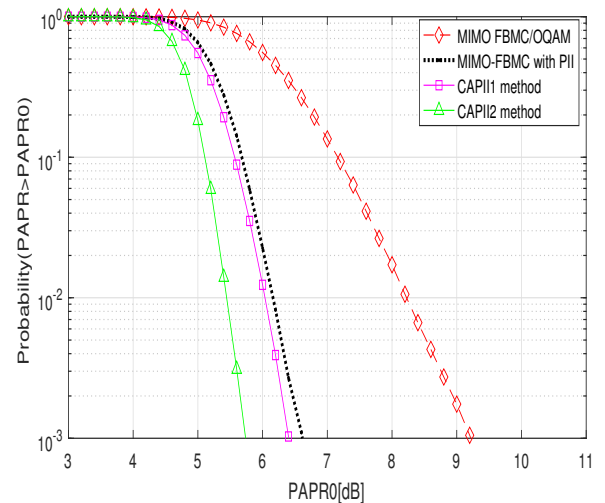


Fig. 5. PAPR reduction capability of both CAPII1 and CAPII2 when applied to SFBC MIMO-FBMC/OQAM signal

TABLE V  
RESULTS OF SIMULATION

PAPR reduction scheme	PII	CAPII1	CAPII2
CCDF at $10^{-3}$ in [dB]	6.6	6.4	5.7

To validate the proposition that FBMC/OQAM stands out as a viable alternative to the OFDM which is the most widespread modulation among all the multicarrier modulations, we conducted simulations incorporating the CAPII1 PAPR reduction scheme within the OFDM system. CCDF plots with both MIMO FBMC/OQAM and MIMO OFDM been shown as depicted in Fig.6.

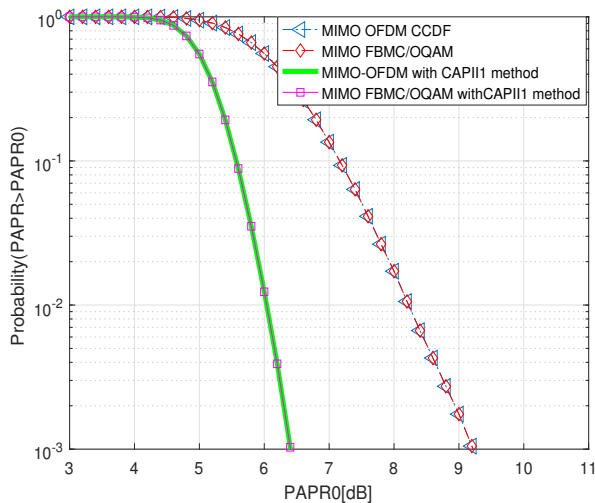


Fig. 6. PAPR reduction capability of CAPII1 when applied to both MIMO-FBMC/OQAM and MIMO-OFDM signals

### B. Computational Complexity:

Computational Complexity consider the computational requirements of the PAPR reduction scheme. Lower complexity is often preferred for practical implementation, as it reduces processing overhead. The being suggested CAPII PAPR reduction schemes for MIMO FBMC/OQAM signal present two different degree of complexity.

When compared to the PII method, the CAPII1 scheme, employing four SFBC patterns, exhibits equivalent complexity. In the case of the CAPII2 scheme, despite its remarkable PAPR reduction, it is characterized by high complexity due to the utilization of eight SFBC patterns.

## V. CONCLUSIONS

This investigation focused on addressing the Peak-to-Average Power Ratio (PAPR) issue in the SFBC MIMO-FBMC/OQAM signal. Consequently, we introduced two novel PAPR reduction schemes, denoted as CAPII1 and CAPII2. Leveraging the additional degrees of freedom provided by multiple antennas, we created four extra cross-antenna SFBC patterns. These patterns formed the basis for designing two

different schemes (CAPII1 and CAPII2). CAPII1 employed only four SFBC patterns for generating candidate signal sets, maintaining the computational complexity equivalent to that of the PII method at both the transmitter and receiver. On the other hand CAPII2 utilized a total of eight SFBC patterns to generate sets of candidate signals for transmission, offering superior PAPR reduction performance albeit with a slightly higher computational complexity. Remarkably, simulation results demonstrated that CAPII1 outperformed the PII method in PAPR reduction despite its comparable computational complexity.

## ACKNOWLEDGMENT

This work was supported by the Innov'COM Laboratory of Higher School of Telecommunication (Sup'Com), University of Carthage Tunisia.

## REFERENCES

- [1] Z. Latinovic and Y. Bar-Ness, "Sfbc mimo-ofdm peak-to-average power ratio reduction by polyphase interleaving and inversion," *IEEE communications letters*, vol. 10, no. 4, pp. 266–268, 2006. [Online]. Available: <https://doi.org/10.1109/LCOMM.2006.1613742>
- [2] S. M. Nejakar, P. G. Benakop, and R. Sharanabasappa, "Orthogonal frequency division multiplexing modulation scheme for 4g/5g cellular network," *European Journal of Advances in Engineering and Technology*, vol. 2, no. 3, pp. 46–50, 2015.
- [3] J. Huang, F. Ruan, M. Su, X. Yang, S. Yao, and J. Zhang, "Analysis of orthogonal frequency division multiplexing (ofdm) technology in wireless communication process," in *2016 10th IEEE International Conference on Anti-counterfeiting, Security, and Identification (ASID)*. IEEE, 2016, pp. 122–125. [Online]. Available: <https://doi.org/10.1109/ICASID.2016.7873931>
- [4] J. Lian, Y. Gao, P. Wu, and D. Lian, "Orthogonal frequency division multiplexing techniques comparison for underwater optical wireless communication systems," *Sensors*, vol. 19, no. 1, p. 160, 2019. [Online]. Available: <https://doi.org/10.3390/s19010160>
- [5] D. Zhang, A. Festag, and G. P. Fettweis, "Performance of generalized frequency division multiplexing based physical layer in vehicular communications," *IEEE Transactions on Vehicular Technology*, vol. 66, no. 11, pp. 9809–9824, 2017. [Online]. Available: <https://doi.org/10.1109/TVT.2017.2723729>
- [6] Y. A. Jawhar, R. A. Abdulhasan, and K. N. Ramli, "Influencing parameters in peak to average power ratio performance on orthogonal frequency-division multiplexing system," *ARNP journal of engineering and applied sciences*, vol. 11, no. 6, pp. 4322–4332, 2016. [Online]. Available: <https://doi.org/10.1109/TELFOR.2014.7034415>
- [7] B. Farhang-Boroujeny, "Filter bank multicarrier modulation: A waveform candidate for 5g and beyond," *Advances in Electrical Engineering*, vol. 2014, 2014. [Online]. Available: <https://doi.org/10.1155/2014/482805>
- [8] D. Levy and A. Reichman, "Filter bank multi carrier modulation performance," in *2017 IEEE International Conference on Microwaves, Antennas, Communications and Electronic Systems (COMCAS)*. IEEE, 2017, pp. 1–6. [Online]. Available: <https://doi.org/10.1109/COMCAS.2017.8244724>
- [9] G. Casu, L. Tută, I. Nicolaescu, and C. Moraru, "Some aspects about the advantages of using mimo systems," in *2014 22nd Telecommunications Forum Telfor (TELFOR)*. IEEE, 2014, pp. 320–323. [Online]. Available: <https://doi.org/10.1109/TELFOR.2014.7034415>
- [10] P. Singh, E. Sharma, K. Vasudevan, and R. Budhiraja, "Cfo and channel estimation for frequency selective mimo-fbmc/oqam systems," *IEEE Wireless Communications Letters*, vol. 7, no. 5, pp. 844–847, 2018. [Online]. Available: <https://doi.org/10.1109/LWC.2018.2830777>
- [11] H. Wang, "Sparse channel estimation for mimo-fbmc/oqam wireless communications in smart city applications," *IEEE Access*, vol. 6, pp. 60666–60672, 2018. [Online]. Available: <https://doi.org/10.1109/ACCESS.2018.2875245>

- [12] Y. Medjahdi, S. Traverso, R. Gerzaguët, H. Shaiek, R. Zayani, D. Demmer, R. Zakaria, J.-B. Doré, M. B. Mabrouk, D. Le Ruyet *et al.*, "On the road to 5g: Comparative study of physical layer in mtc context," *IEEE Access*, vol. 5, pp. 26 556–26 581, 2017. [Online]. Available: <https://doi.org/10.1109/ACCESS.2017.2774002>
- [13] J. Nadal, C. A. Nour, and A. Baghdadi, "Design and evaluation of a novel short prototype filter for fbmc/oqam modulation," *IEEE access*, vol. 6, pp. 19 610–19 625, 2018. [Online]. Available: <https://doi.org/10.1109/ACCESS.2018.2818883>
- [14] R. Nissel, S. Schwarz, and M. Rupp, "Filter bank multicarrier modulation schemes for future mobile communications," *IEEE Journal on Selected Areas in Communications*, vol. 35, no. 8, pp. 1768–1782, 2017. [Online]. Available: <https://doi.org/10.1109/JSAC.2017.2710022>
- [15] A. Skrzypczak, J. Palicot, and P. Siohan, "Ofdm/oqam modulation for efficient dynamic spectrum access," *International Journal of Communication Networks and Distributed Systems*, vol. 8, no. 3–4, pp. 247–266, 2012. [Online]. Available: <https://doi.org/10.1504/IJCND.2012.046360>
- [16] A. Boudjelkha, H. Merah, and A. Khelil, "Multi-antennas papr reduction for fbmc/oqam system," *International Journal of Sensors Wireless Communications and Control*, vol. 13, no. 2, pp. 108–116, 2023. [Online]. Available: <https://doi.org/10.2174/2210327913666230512163935>
- [17] A. Agarwal and R. Sharma, "Review of different papr reduction techniques in fbmc-oqam system," *Internet of Things and Big Data Applications: Recent Advances and Challenges*, pp. 183–191, 2020. [Online]. Available: [https://doi.org/DOI:10.1007/978-3-030-39119-5\\_14](https://doi.org/DOI:10.1007/978-3-030-39119-5_14)
- [18] H. Wang, X. Wang, L. Xu, and W. Du, "Hybrid papr reduction scheme for fbmc/oqam systems based on multi data block pts and tr methods," *IEEE Access*, vol. 4, pp. 4761–4768, 2016. [Online]. Available: <https://doi.org/10.1109/ACCESS.2016.2605008>
- [19] X. Cheng, D. Liu, W. Shi, Y. Zhao, Y. Li, and D. Kong, "A novel conversion vector-based low-complexity slm scheme for papr reduction in fbmc/oqam systems," *IEEE Transactions on Broadcasting*, vol. 66, no. 3, pp. 656–666, 2020. [Online]. Available: <https://doi.org/10.1109/TBC.2020.2977548>
- [20] M. Laabidi, R. Zayani, D. Roviras, and R. Bouallegue, "Papr reduction in fbmc/oqam systems using active constellation extension and tone reservation approaches," in *2015 IEEE Symposium on Computers and Communication (ISCC)*. IEEE, 2015, pp. 657–662. [Online]. Available: <https://doi.org/10.1109/ISCC.2015.7405589>
- [21] M. Laabidi and R. Bouallegue, "Three implementations of the tone reservation papr reduction scheme for the fbmc/oqam system," *IET Communications*, vol. 13, no. 7, pp. 918–925, 2019. [Online]. Available: <https://doi.org/10.1049/iet-com.2018.5336>
- [22] R. Gopal and S. K. Patra, "Combining tone injection and companding techniques for papr reduction of fbmc-oqam system," in *2015 Global Conference on Communication Technologies (GCCT)*. IEEE, 2015, pp. 709–713. [Online]. Available: <https://doi.org/10.1109/GCCT.2015.7342756>
- [23] X. Liu, X. Ge, H. Zhou, T. He, and G. Qiao, "Papr reduction for fbmc-oqam system with laplace based linear companding transform," *IEEE Communications Letters*, 2023. [Online]. Available: <https://doi.org/10.1109/LCOMM.2023.3335911>
- [24] I. A. Shaheen, A. Zekry, F. Newagy, and R. Ibrahim, "Papr reduction of fbmc/oqam systems based on combination of dst precoding and a-law nonlinear companding technique," in *2017 International Conference on Promising Electronic Technologies (ICPET)*. IEEE, 2017, pp. 38–42. [Online]. Available: <https://doi.org/10.1109/ICPET.2017.13>
- [25] —, "Proposed new schemes to reduce papr for stbc mimo fbmc systems," *simulation*, vol. 6, no. 9, 2017.
- [26] H. Merah, M. Mesri, K. Tahkoubit, and L. Talbd, "Papr reduction in mimo (2x2)-fbmc-oqam systems using attenuating qam symbols," in *2019 6th International Conference on Image and Signal Processing and their Applications (ISPA)*, 2019, pp. 1–5. [Online]. Available: <https://doi.org/10.1109/ISPA48434.2019.8966794>
- [27] I. A. Shaheen, A. Zekry, F. Newagy, and R. Ibrahim, "Papr reduction using combination of sas preprocessed and wht precoding for mimo system of fbmc/oqam transceiver," *International Journal of Engineering & Technology*, vol. 7, no. 4, pp. 3803–3809, 2018. [Online]. Available: <https://doi.org/10.14419/ijet.v7i4.15899>
- [28] A. Boudjelkha, A. Khelil, and H. Merah, "Repeated clipping filtering with nonlinear companding for papr reduction in mimo fbmc/oqam system," *International Journal of Intelligent Engineering & Systems*, vol. 16, no. 4, 2023. [Online]. Available: <https://doi.org/10.22266/ijies2023.0831.51>
- [29] A. Sahin, I. Guvenc, and H. Arslan, "A survey on multicarrier communications: Prototype filters, lattice structures, and implementation aspects," *IEEE communications surveys & tutorials*, vol. 16, no. 3, pp. 1312–1338, 2013. [Online]. Available: <https://doi.org/10.1109/SURV.2013.121213.00263>
- [30] deliverable 2.1, "Transmit/receive processing (single antenna)," *document ICT-211887 PHYDYAS*, vol. Jul, 2008.
- [31] J. Nadal, C. A. Nour, A. Baghdadi, and H. Lin, "Hardware prototyping of fbmc/oqam baseband for 5g mobile communication systems," in *RSP 2014: IEEE International Symposium on Rapid System Prototyping*, 2014, pp. 135–141.
- [32] M. Bellanger, "Physical layer for future broadband radio systems," in *2010 IEEE radio and wireless symposium (RWS)*. IEEE, 2010, pp. 436–439. [Online]. Available: <https://doi.org/10.1109/RWS.2010.5434093>
- [33] S. S. K. C. Bulusu, "Performance analysis and papr reduction techniques for filter-bank based multi-carrier systems with non-linear power amplifiers," Ph.D. dissertation, Conservatoire national des arts et metiers-CNAM, 2016.
- [34] S. M. Alamouti, "A simple transmit diversity technique for wireless communications," *IEEE Journal on selected areas in communications*, vol. 16, no. 8, pp. 1451–1458, 1998.